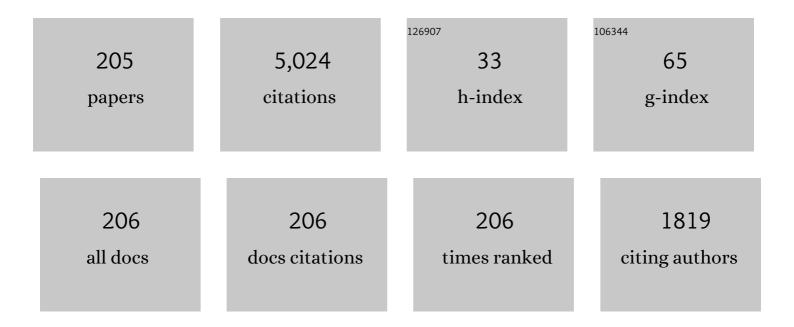
List of Publications by Year in descending order

Source: https://exaly.com/author-pdf/1353516/publications.pdf Version: 2024-02-01



#	Article	IF	CITATIONS
1	Photoelectrochemical properties of plasma-induced nanostructured tungsten oxide. Applied Surface Science, 2022, 580, 151979.	6.1	10
2	Nitrogen Atom Density Measurements in NAGDIS-T Using Vacuum Ultraviolet Absorption Spectroscopy. Plasma and Fusion Research, 2022, 17, 1201004-1201004.	0.7	0
3	An approach to implement a heat flux limit in a model for fusion relevant plasmas. Physics of Plasmas, 2022, 29, .	1.9	1
4	Changes in morphology and field emission property of nano-tendril bundles after high temperature annealing. Nuclear Materials and Energy, 2022, 31, 101178.	1.3	6
5	lsotope Effect for Plasma Detachment in Helium and Hydrogen/Deuterium Mixture Plasmas. Plasma and Fusion Research, 2022, 17, 2402027-2402027.	0.7	0
6	Measurement of the Bidirectional Reflectance Distribution Function of Tungsten Surface Sputtered in Argon Plasma. Plasma and Fusion Research, 2022, 17, 2405041-2405041.	0.7	4
7	Nano-tendril bundles behavior under plasma-relevant electric fields. Vacuum, 2021, 183, 109799.	3.5	5
8	Doppler and Stark Broadenings of He II Emission in NAGDIS-PG. Plasma and Fusion Research, 2021, 16, 1202013-1202013.	0.7	0
9	Fabrication of nanostructured Ti thin film with Ti deposition in He plasmas. Japanese Journal of Applied Physics, 2021, 60, 038004.	1.5	7
10	Influence of Nitrogen Ratio on Plasma Detachment during Combined Seeding with Hydrogen on Divertor Simulation Experiment of GAMMA 10/PDX. Plasma and Fusion Research, 2021, 16, 2402041-2402041.	0.7	4
11	Computer Tomography on Divertor Impurity Monitor for ITER with Minimizing Errors in a Logarithmic Scale. Plasma and Fusion Research, 2021, 16, 2405019-2405019.	0.7	7
12	Modeling of the impurity-induced silicon nanocone growth by low energy helium plasma irradiation. Plasma Science and Technology, 2021, 23, 045503.	1.5	2
13	Accelerated/reduced growth of tungsten fuzz by deposition of metals. Journal of Nuclear Materials, 2021, 548, 152844.	2.7	18
14	Enhancement of Arc Ignition on Tungsten in Helium Plasmas with Impurity Gases. Plasma and Fusion Research, 2021, 16, 2405069-2405069.	0.7	5
15	Thermal treatment of W large-scale fiberform nanostructures. Physica Scripta, 2021, 96, 094004.	2.5	1
16	The dependence of Mo ratio on the formation of uniform black silicon by helium plasma irradiation. Journal Physics D: Applied Physics, 2021, 54, 405202.	2.8	6
17	Enhanced photocatalytic ethylene decomposition with anatase-rutile mixed nanostructures formed by He plasma treatment. Journal of Photochemistry and Photobiology A: Chemistry, 2021, 418, 113420.	3.9	9
18	Tungsten Large-Scale Fiberform Nanostructures Retained under High Temperature Conditions. Plasma and Fusion Research, 2021, 16, 1206001-1206001.	0.7	2

#	Article	IF	CITATIONS
19	Overheating of Nanostructured Tendril Bundles due to Thermo-Field Emission. , 2021, , .		0
20	Growth of Mo Large-Scale Fiberform Nanostructures. Plasma and Fusion Research, 2021, 16, 1206105-1206105.	0.7	2
21	Photocatalytic application of helium plasma induced nanostructured tungsten oxides. Japanese Journal of Applied Physics, 2020, 59, SAAB04.	1.5	5
22	Detached helium plasma simulation by a one-dimensional fluid code with detailed collisional-radiative model. Physics of Plasmas, 2020, 27, 102505.	1.9	10
23	Helium-W co-deposition layer: TEM observation and D retention. Journal of Nuclear Materials, 2020, 540, 152350.	2.7	6
24	The influence of impurities on the formation of nanocone structures on silicon surface irradiated by low energy helium plasma. Journal of Applied Physics, 2020, 128, .	2.5	7
25	Effect of temperature and incident ion energy on nanostructure formation on silicon exposed to helium plasma. Plasma Processes and Polymers, 2020, 17, 2000126.	3.0	5
26	Evaluation of axial decay length of plasma pressure in detached plasma. Nuclear Materials and Energy, 2020, 25, 100812.	1.3	1
27	Tungsten fuzz: Deposition effects and influence to fusion devices. Nuclear Materials and Energy, 2020, 25, 100828.	1.3	15
28	Size distribution of nano-tendril bundles with various additional impurity gases. Nuclear Materials and Energy, 2020, 25, 100843.	1.3	2
29	Inspection of Arc Trails Formed in Stellarator/Heliotron Devices W7-X and LHD. Plasma and Fusion Research, 2020, 15, 2402012-2402012.	0.7	5
30	First EMC3â€EIRENE modelling of JTâ€60SA edge plasmas with/without resonant magnetic perturbation field. Contributions To Plasma Physics, 2020, 60, e201900114.	1.1	0
31	Spatiotemporal dynamics of cross-field ejection events in recombining detached plasma. Plasma Physics and Controlled Fusion, 2020, 62, 075011.	2.1	9
32	Microstructure and Retention in He-W Co-Deposition Layer. Plasma and Fusion Research, 2020, 15, 1201004-1201004.	0.7	5
33	Application of dynamic mode decomposition to rotating structures in detached linear plasmas. Physics of Plasmas, 2020, 27, .	1.9	7
34	Unipolar arc plasmas on nanostructured tungsten surfaces under perpendicular magnetic field. Plasma Sources Science and Technology, 2020, 29, 125015.	3.1	7
35	Dust Formation from Arc Spots on Nanostructured Tungsten Surface. Plasma and Fusion Research, 2020, 15, 1205061-1205061.	0.7	3
36	Thin film and noble metal loading effects on the photocatalytic reactivity of helium-plasma-induced nanostructured tungsten oxides. Materials Research Express, 2020, 7, 075007.	1.6	5

#	Article	IF	CITATIONS
37	Plasma Potential Measurement in Detached Plasmas by Emissive Probe Considering Space-Charge-Limited Effect. Plasma and Fusion Research, 2020, 15, 1301082-1301082.	0.7	1
38	Dynamics of Hydrogen Isotope Absorption and Emission of Neutron-Irradiated Tungsten. Plasma and Fusion Research, 2020, 15, 1505081-1505081.	0.7	3
39	Photocatalytic decomposition of ethylene using He plasma induced nano-TiO ₂ . Japanese Journal of Applied Physics, 2019, 58, 070903.	1.5	7
40	Generation of Spiral Shape Nitrogen Recombining Plasma for Atomic Nitrogen Source. Plasma and Fusion Research, 2019, 14, 3401069-3401069.	0.7	3
41	Spatial and temporal measurement of recombining detached plasmas by laser Thomson scattering. Plasma Sources Science and Technology, 2019, 28, 105015.	3.1	7
42	Field Emission From Nanostructured Tendril Bundles. IEEE Transactions on Plasma Science, 2019, 47, 5186-5190.	1.3	17
43	Development of Thomson Scattering Measurement System for Upstream Plasmas in the NAGDIS-II Device. Plasma and Fusion Research, 2019, 14, 2405031-2405031.	0.7	5
44	Influence of heavier impurity deposition on surface morphology development and sputtering behavior explored in multiple linear plasma devices. Nuclear Materials and Energy, 2019, 18, 67-71.	1.3	14
45	Characterization of He Induced Nanostructures Using SEM Image Analysis . Plasma and Fusion Research, 2019, 14, 3402049-3402049.	0.7	1
46	Helium-plasma–induced straight nanofiber growth on HCP metals. Acta Materialia, 2019, 181, 342-351.	7.9	15
47	Fabrication of a nanostructured TiO ₂ photocatalyst using He plasma-irradiated tungsten and ethylene gas decomposition. Japanese Journal of Applied Physics, 2019, 58, SEEG01.	1.5	10
48	Investigation of recombination front region in detached plasmas in a linear divertor plasma simulator. Nuclear Materials and Energy, 2019, 19, 458-462.	1.3	23
49	Ignition and Behavior of Arc Spots on Helium Irradiated Tungsten Under Fusion Relevant Condition. IEEE Transactions on Plasma Science, 2019, 47, 3609-3616.	1.3	9
50	lgnition and Sustainment of Arcing on Nanostructured Tungsten Under Plasma Exposure. IEEE Transactions on Plasma Science, 2019, 47, 3617-3625.	1.3	9
51	Doubleâ€probe measurement in recombining plasma using NACDISâ€II. Contributions To Plasma Physics, 2019, 59, e201800088.	1.1	5
52	Multipoint measurements employing a microwave interferometer and a Langmuir probe in the detached linear plasma. AIP Advances, 2019, 9, 015016.	1.3	5
53	Spatiotemporal Structure of Hl $^{\rm t}$ Emission from the Detached Plasma in GAMMA 10/PDX. Plasma and Fusion Research, 2019, 14, 2402036-2402036.	0.7	2
54	Increased Energy Absorption into W due to the Metal Deposited Layer from an ELM-like Pulsed Plasma. Plasma and Fusion Research, 2019, 14, 1401051-1401051.	0.7	1

#	Article	IF	CITATIONS
55	Application of Ion Sensitive Probe to High Density Plasmas in Magnum-PSI. Plasma and Fusion Research, 2019, 14, 1202135-1202135.	0.7	5
56	Fabrication of photocatalytically active vanadium oxide nanostructures via plasma route. Journal Physics D: Applied Physics, 2018, 51, 215201.	2.8	20
57	Fuzzy nanostructure growth on precious metals by He plasma irradiation. Surface and Coatings Technology, 2018, 340, 86-92.	4.8	31
58	Measurement of He neutral temperature in detached plasmas using laser absorption spectroscopy. AIP Advances, 2018, 8, .	1.3	4
59	Enhanced growth of large-scale nanostructures with metallic ion precipitation in helium plasmas. Scientific Reports, 2018, 8, 56.	3.3	60
60	Pulsation Effects of Incident Ion Energy on W Fuzz Growth. Plasma and Fusion Research, 2018, 13, 1205001-1205001.	0.7	6
61	Mode Structure Analysis of Detached Plasmas with 2D Images. Plasma and Fusion Research, 2018, 13, 1402033-1402033.	0.7	3
62	Thomson Scattering Measurement of Two Electron Temperature Components in Transition to Detached Plasmas. Plasma and Fusion Research, 2018, 13, 1201099-1201099.	0.7	6
63	Morphology Changes of Platinum and Tungsten Carbide by He Plasma Irradiation. Plasma and Fusion Research, 2018, 13, 3406074-3406074.	0.7	0
64	Ignition and Sustainment of Arcing on Nanostructured Tungsten under Plasma Exposure. , 2018, , .		1
65	Emission from Tungsten Nanostructured Tendril Bundles under Local Thermal Load. , 2018, , .		Ο
66	One‣tep Plasma Synthesis of Nb ₂ O ₅ Nanofibers and their Enhanced Photocatalytic activity. ChemPhysChem, 2018, 19, 3237-3246.	2.1	11
67	Blob- and hole-like structures outstanding during the transition from attached to detached divertor states in GAMMA 10/PDX. Physics of Plasmas, 2018, 25, 082505.	1.9	4
68	Effect of the Nanostructured Layer Thickness on the Dynamics of Cathode Spots on Tungsten. IEEE Transactions on Plasma Science, 2018, 46, 4044-4050.	1.3	11
69	lgnition and erosion of materials by arcing in fusionâ€relevant conditions. Contributions To Plasma Physics, 2018, 58, 608-615.	1.1	23
70	Helium line emission spectroscopy in recombining detached plasmas. Physics of Plasmas, 2018, 25, 063303.	1.9	18
71	Localized spiraling plasma ejection contributing the ion-flux broadening in the detached linear plasma. Plasma Physics and Controlled Fusion, 2018, 60, 075013.	2.1	18
72	Morphologies of co-depositing W layer formed during He plasma irradiation. Nuclear Fusion, 2018, 58, 106002.	3.5	22

#	Article	IF	CITATIONS
73	Growth of nano-tendril bundles on tungsten with impurity-rich He plasmas. Nuclear Fusion, 2018, 58, 096022.	3.5	40
74	Nanostructure Growth on Rhodium/Ruthenium by the Exposure to He Plasma. Plasma and Fusion Research, 2018, 13, 3406065-3406065.	0.7	2
75	Tailoring of fuzzy nanostructures on porous tungsten skeleton by helium plasma irradiation. Japanese Journal of Applied Physics, 2017, 56, 030303.	1.5	6
76	Plasma detachment in linear devices. Plasma Physics and Controlled Fusion, 2017, 59, 034007.	2.1	80
77	Fractality and growth of He bubbles in metals. Physics Letters, Section A: General, Atomic and Solid State Physics, 2017, 381, 2355-2362.	2.1	17
78	Field Emission From Metal Surfaces Irradiated With Helium Plasmas. IEEE Transactions on Plasma Science, 2017, 45, 2080-2086.	1.3	33
79	Erosion of nanostructured tungsten by laser ablation, sputtering and arcing. Nuclear Materials and Energy, 2017, 12, 386-391.	1.3	26
80	Transverse motion of a plasma column in a sheet plasma. Contributions To Plasma Physics, 2017, 57, 87-93.	1.1	10
81	Studies of power exhaust and divertor design for a 1.5 GW-level fusion power DEMO. Nuclear Fusion, 2017, 57, 126050.	3.5	65
82	Extension of the operational regime of the LHD towards a deuterium experiment. Nuclear Fusion, 2017, 57, 102023.	3.5	116
83	Molecular activated recombination in divertor simulation plasma on GAMMA 10/PDX. Nuclear Materials and Energy, 2017, 12, 1004-1009.	1.3	32
84	Influence of expanding and contracting magnetic field configurations on detached plasma formation in a linear plasma device. Physics of Plasmas, 2017, 24, .	1.9	5
85	Behavior of 23S metastable state He atoms in low-temperature recombining plasmas. Physics of Plasmas, 2017, 24, 073301.	1.9	19
86	Measurement of Poloidal Flow Profiles Using a Mach Probe Array in HYBTOK-II Tokamak with RMP Fields. Plasma and Fusion Research, 2017, 12, 1202027-1202027.	0.7	0
87	Development of a Compact Divertor Plasma Simulator for Plasma-Wall Interaction Studies on Neutron-Irradiated Materials. Plasma and Fusion Research, 2017, 12, 1405040-1405040.	0.7	8
88	Localized Density Fluctuation in the Downstream of Detached Plasma. Plasma and Fusion Research, 2017, 12, 1202007-1202007.	0.7	8
89	Modeling of Linear Divertor Plasma Simulator Experiments with Threeâ€dimensional Target Structure by Using EMC3â€EIRENE Code. Contributions To Plasma Physics, 2016, 56, 598-603.	1.1	2
90	Effect of nanostructured layer thickness on tungsten surface on cathode spots dynamics. , 2016, , .		0

#	Article	IF	CITATIONS
91	Measurement of heat diffusion across fuzzy tungsten layer. Results in Physics, 2016, 6, 877-878.	4.1	48
92	Enhancement of photocatalytic activity of TiO ₂ by plasma irradiation. Japanese Journal of Applied Physics, 2016, 55, 106202.	1.5	7
93	Investigation of arcing on fiber-formed nanostructured tungsten by pulsed plasma during steady state plasma irradiation. Fusion Engineering and Design, 2016, 112, 156-161.	1.9	21
94	Photon Trapping Effects in DEMO Divertor Plasma. Contributions To Plasma Physics, 2016, 56, 657-662.	1.1	11
95	Fuzzy nanostructure growth on Ta/Fe by He plasma irradiation. Scientific Reports, 2016, 6, 30380.	3.3	47
96	Strong Reduction of Ion Flux to a Target Plate in a Magnetically Contracting Detached Plasma. Plasma and Fusion Research, 2016, 11, 1202005-1202005.	0.7	4
97	Field electron emission from metal surfaces irradiated with helium plasmas. , 2016, , .		1
98	Vacuum breakdown from nanostructured fuzzy surfaces. , 2016, , .		2
99	Statistical Analysis of Particle Flux Flowing into the Endâ€Target in between Attached and Detached States in the Linear Divertor Plasma Simulator NAGDISâ€II. Contributions To Plasma Physics, 2016, 56, 723-728.	1.1	4
100	Detailed Analysis of Plasma Resistivity in Detached Recombining Plasmas. Contributions To Plasma Physics, 2016, 56, 717-722.	1.1	2
101	Influence of Deuterium Retention on Secondary Electron Emission from Graphite under Deuterium Plasma Exposure. Plasma and Fusion Research, 2015, 10, 1402009-1402009.	0.7	1
102	Morphology and Optical Property Changes of Nanostructured Tungsten in LHD. Plasma and Fusion Research, 2015, 10, 1402083-1402083.	0.7	2
103	Correlation Analysis of 3–4 Kilohertz Core and Edge Density Fluctuations in the GAMMA 10 Tandem Mirror Device. Fusion Science and Technology, 2015, 68, 125-129.	1.1	1
104	Sulfur K-edge XANES for methylene blue in photocatalytic reaction over WO3 nanomaterials. Nuclear Instruments & Methods in Physics Research B, 2015, 365, 35-38.	1.4	23
105	Hybrid simulation research on formation mechanism of tungsten nanostructure induced by helium plasma irradiation. Journal of Nuclear Materials, 2015, 463, 109-115.	2.7	48
106	Growth of multifractal tungsten nanostructure by He bubble induced directional swelling. New Journal of Physics, 2015, 17, 043038.	2.9	57
107	Increase in the work function of W/WO ₃ by helium plasma irradiation. Japanese Journal of Applied Physics, 2015, 54, 126201.	1.5	10
108	Application of Nanostructured Tungsten Fabricated by Helium Plasma Irradiation for Photoinduced Decolorization of Methylene Blue. E-Journal of Surface Science and Nanotechnology, 2014, 12, 343-348.	0.4	12

#	Article	IF	CITATIONS
109	Thermal response of nanostructured tungsten. Nuclear Fusion, 2014, 54, 033005.	3.5	66
110	A plasma source driven predator-prey like mechanism as a potential cause of spiraling intermittencies in linear plasma devices. Physics of Plasmas, 2014, 21, 032302.	1.9	15
111	Compact and high-particle-flux thermal-lithium-beam probe system for measurement of two-dimensional electron density profile. Review of Scientific Instruments, 2014, 85, 093510.	1.3	0
112	Surface modification of titanium using He plasma. Applied Surface Science, 2014, 303, 438-445.	6.1	41
113	In situ observation of structural change of nanostructured tungsten during annealing. Journal of Nuclear Materials, 2014, 449, 9-14.	2.7	56
114	Influence of Plasma-Neutral Collisions on Probe Measurements in Atmospheric Pressure Plasmas. Contributions To Plasma Physics, 2014, 54, 304-307.	1.1	3
115	Fractality of self-grown nanostructured tungsten by He plasma irradiation. Physics Letters, Section A: General, Atomic and Solid State Physics, 2014, 378, 2533-2538.	2.1	24
116	Transition in velocity and grouping of arc spot on different nanostructured tungsten electrodes. Results in Physics, 2014, 4, 33-39.	4.1	27
117	Helium plasma irradiation on single crystal tungsten and undersized atom doped tungsten alloys. Physica Scripta, 2014, 89, 025602.	2.5	25
118	Current Activities in the Interactive Joint Research at Tohoku University - Advanced Evaluation of Radiation Effects on Fusion Materials Plasma and Fusion Research, 2014, 9, 3405136-3405136.	0.7	3
119	Helium effects on tungsten surface morphology and deuterium retention. Journal of Nuclear Materials, 2013, 442, S267-S272.	2.7	83
120	Observation of Arc Spots Initiated on Nanostructured Tungsten. IEEE Transactions on Plasma Science, 2013, 41, 1889-1895.	1.3	7
121	Helium plasma implantation on metals: Nanostructure formation and visible-light photocatalytic response. Journal of Applied Physics, 2013, 113, .	2.5	88
122	Growth annealing equilibrium of tungsten nanostructures by helium plasma irradiation in non-eroding regimes. Journal of Nuclear Materials, 2013, 440, 55-62.	2.7	44
123	Characterization of Gun Plasma Penetrated Into a Steady State Plasma Device. IEEE Transactions on Plasma Science, 2013, 41, 3122-3128.	1.3	1
124	Influence of crystal orientation on damages of tungsten exposed to helium plasma. Journal of Nuclear Materials, 2013, 438, S879-S882.	2.7	87
125	Influence of the Probe Electrode on Probe Measurements for Atmospheric Pressure Microwave Plasma Torch. Contributions To Plasma Physics, 2013, 53, 81-85.	1.1	0
126	Tritium retention in nanostructured tungsten with large effective surface area. Journal of Nuclear Materials, 2013, 438, S1142-S1145.	2.7	29

#	Article	IF	CITATIONS
127	Low-energy helium irradiation on in-vessel mirror materials. Journal of Nuclear Materials, 2013, 442, S515-S519.	2.7	4
128	Development of steady/transient dual plasma irradiation device using a plasma gun. Journal of Nuclear Materials, 2013, 438, S707-S710.	2.7	6
129	Field emission property of nanostructured tungsten formed by helium plasma irradiation. Fusion Engineering and Design, 2013, 88, 2842-2847.	1.9	33
130	Impact of arcing on carbon and tungsten: from the observations in JT-60U, LHD and NAGDIS-II. Nuclear Fusion, 2013, 53, 053013.	3.5	41
131	Effect of resistivity profile on current decay time of initial phase of current quench in neon-gas-puff inducing disruptions of JT-60U. Physics of Plasmas, 2013, 20, 112507.	1.9	2
132	Spectroscopic Study and Motion Analysis of Arc Spot Initiated on Nanostructured Tungsten. Japanese Journal of Applied Physics, 2013, 52, 11NC02.	1.5	11
133	Comparison of Damages on Tungsten Surface Exposed to Noble Gas Plasmas. Plasma Science and Technology, 2013, 15, 282-286.	1.5	33
134	Power Transmission Factor for Tungsten Target w/wo Fiber-Form Nanostructure in He Plasmas with Hot Electron Component Using Compact Plasma Device AIT-PID. Fusion Science and Technology, 2013, 63, 225-228.	1.1	15
135	Behavior of Plasma Response Field in Detached Plasma. Plasma and Fusion Research, 2013, 8, 1402058-1402058.	0.7	11
136	Arcing on tungsten subjected to helium and transients: ignition conditions and erosion rates. Plasma Physics and Controlled Fusion, 2012, 54, 035009.	2.1	44
137	Statistical Analysis of the Spatial Behavior of Plasma Blobs Around the Plasma Column in a Linear Plasma Device. Contributions To Plasma Physics, 2012, 52, 424-428.	1.1	17
138	Conditions for the Release of a Metallic Dust Particle from a Plasma-Facing Wall. Contributions To Plasma Physics, 2012, 52, 478-483.	1.1	2
139	Blob/Hole Generation in the Divertor Leg of the Large Helical Device. Plasma and Fusion Research, 2012, 7, 1402152-1402152.	0.7	6
140	Thermionic Energy Converter System Using Heat Flux in Divertor Region. Plasma and Fusion Research, 2012, 7, 1405050-1405050.	0.7	2
141	Superimposition of Pulses to Steady Arc Discharge in Toroidal Divertor Simulator. Plasma and Fusion Research, 2012, 7, 1405100-1405100.	0.7	1
142	Fatal Damages due to Breakdown on a Diagnostic Mirror Located outside the Vacuum Vessel in JT-60U. Plasma and Fusion Research, 2012, 7, 2405121-2405121.	0.7	2
143	Effect of Externally Applied Resonance Magnetic Perturbation on Current Decay during Tokamak Disruption. Plasma and Fusion Research, 2012, 7, 1202049-1202049.	0.7	0
144	TEM observation of the growth process of helium nanobubbles on tungsten: Nanostructure formation mechanism. Journal of Nuclear Materials, 2011, 418, 152-158.	2.7	226

#	Article	IF	CITATIONS
145	Development of Nanostructured Black Metal by Self-Growing Helium Bubbles for Optical Application. Japanese Journal of Applied Physics, 2011, 50, 08JG01.	1.5	11
146	Formation and decay processes of Ar/He microwave plasma jet at atmospheric gas pressure. Journal of Applied Physics, 2011, 110, .	2.5	24
147	Exfoliation of the tungsten fibreform nanostructure by unipolar arcing in the LHD divertor plasma. Nuclear Fusion, 2011, 51, 102001.	3.5	73
148	Motion of unipolar arc spots ignited on a nanostructured tungsten surface. Plasma Physics and Controlled Fusion, 2011, 53, 074002.	2.1	24
149	Deuterium Uptake in Iron Oxide (Fe[sub 2]O[sub 3]) Under D[sub 2]+]-Plasma Exposure. , 2011, , .		0
150	Study of Plasma Current Decay in the Initial Phase of High Poloidal Beta Disruptions in JT-60U. Plasma and Fusion Research, 2011, 6, 1302136-1302136.	0.7	8
151	OS20-2-4 Warpage of Si/Solder/OFHC-Cu Layered Structures Subjected to Cyclic Thermal Loading. The Abstracts of ATEM International Conference on Advanced Technology in Experimental Mechanics Asian Conference on Experimental Mechanics, 2011, 2011.10, _OS20-2-4	0.0	0
152	2D Measurement of Edge Plasma Dynamics by Using High‣peed Camera Based on Hel Line Intensity Ratio Method. Contributions To Plasma Physics, 2010, 50, 962-969.	1.1	12
153	2D Statistical Analysis of Nonâ€Ðiffusive Transport under Attached and Detached Plasma Conditions of the Linear Divertor Simulator. Contributions To Plasma Physics, 2010, 50, 256-266.	1.1	34
154	Formation Condition of Fiberform Nanostructured Tungsten by Helium Plasma Exposure. Plasma and Fusion Research, 2010, 5, S1023-S1023.	0.7	21
155	Deepening of Floating Potential for Tungsten Target Plate on the way to Nanostructure Formation. Plasma and Fusion Research, 2010, 5, 039-039.	0.7	25
156	Enhancement of cross-field transport into the private region of detached-divertor in Large Helical Device. Physics of Plasmas, 2010, 17, 102509.	1.9	27
157	Nanostructured Black Metal: Novel Fabrication Method by Use of Self-Growing Helium Bubbles. Applied Physics Express, 2010, 3, 085204.	2.4	77
158	Self-Affine Fractality of Bifurcating Arc Trail in Magnetized Plasma. Journal of the Physical Society of Japan, 2010, 79, 054501.	1.6	14
159	Fluid Mechanical Characteristics of Microwave Discharge Jet Plasmas at Atmospheric Gas Pressure. IEEJ Transactions on Fundamentals and Materials, 2010, 130, 493-500.	0.2	5
160	Comparison of Hydrogen Adsorption on Diamond and Graphite Surfaces. Plasma and Fusion Research, 2010, 5, S2072-S2072.	0.7	1
161	Visualized Blow-off from Helium Irradiated Tungsten in Response to ELM-like Heat Load. Plasma and Fusion Research, 2009, 4, 004-004.	0.7	33
162	Flattening-induced electronic changes in zigzag single- and multi-walled boron nitride nanotubes: A first-principles DFT study. Physical Review B, 2009, 80, .	3.2	12

#	Article	IF	CITATIONS
163	Ray tracing simulation for radiation trapping of the He I resonance transitions in a linear plasma device. Physics of Plasmas, 2009, 16, .	1.9	13
164	Formation and mitigation of fiberform nanostructured tungsten by helium and sub-ms laser pulse irradiations. Plasma Devices and Operations, 2009, 17, 165-173.	0.6	2
165	Development of Divertor Plasma Simulators with High Heat Flux Plasmas and its Application to Nuclear Fusion Study: A Review. IEEJ Transactions on Electrical and Electronic Engineering, 2009, 4, 476-487.	1.4	1
166	Direct observation of cathode spot grouping using nanostructured electrode. Physics Letters, Section A: General, Atomic and Solid State Physics, 2009, 373, 4273-4277.	2.1	24
167	Prompt ignition of a unipolar arc on helium irradiated tungsten. Nuclear Fusion, 2009, 49, 032002.	3.5	105
168	Formation process of tungsten nanostructure by the exposure to helium plasma under fusion relevant plasma conditions. Nuclear Fusion, 2009, 49, 095005.	3.5	494
169	Sub-ms laser pulse irradiation on tungsten target damaged by exposure to helium plasma. Nuclear Fusion, 2007, 47, 1358-1366.	3.5	180
170	Formation of Nanostructured Tungsten with Arborescent Shape due to Helium Plasma Irradiation. Plasma and Fusion Research, 2006, 1, 051-051.	0.7	375
171	Reduction of laser power threshold for melting tungsten due to subsurface helium holes. Journal of Applied Physics, 2006, 100, 103304.	2.5	37
172	Recent Results in Divertor Plasma Simulators. Journal of Plasma and Fusion Research, 2004, 80, 212-216.	0.4	5
173	Visualization of Intermittent Blobby Plasma Transport in Attached and Detached Plasmas of the NAGDIS-II. Journal of Plasma and Fusion Research, 2004, 80, 275-276.	0.4	24
174	Transition from electrostatic-to-electromagnetic mode in a radio-frequency Ar inductively coupled plasma in atmospheric pressure. Journal of Applied Physics, 2004, 95, 427-433.	2.5	29
175	On the Acoustic Nonlinearity of Solid-Solid Contact With Pressure-Dependent Interface Stiffness. Journal of Applied Mechanics, Transactions ASME, 2004, 71, 508-515.	2.2	189
176	Space-Charge Limited Current from Plasma-Facing Material Surface. Contributions To Plasma Physics, 2004, 44, 126-137.	1.1	123
177	Proposal of Modified Child-Langmuir Formula describing Space-Charge Limited Current in Plasma. Contributions To Plasma Physics, 2004, 44, 144-149.	1.1	13
178	Reconstruction of Velocity Distribution of Density Bursts by Wavelet Analysis in the Linear Divertor Simulator NAGDIS-II. Contributions To Plasma Physics, 2004, 44, 222-227.	1.1	28
179	Intermittent Structures in the High Field Side Boundary of the HYBTOK-II Tokamak. European Physical Journal D, 2003, 53, 863-868.	0.4	2
180	Formation and Dynamics of Very Deep Negative Potential Well in the Small Tokamak Device CSTN-IV. European Physical Journal D, 2003, 53, 895-902.	0.4	0

#	Article	IF	CITATIONS
181	Sound Wave Propagation in Gases at Low Pressure. AIP Conference Proceedings, 2003, , .	0.4	1
182	COMPUTATIONAL MODELING OF WAVE SCATTERING IN FIBER REINFORCED COMPOSITE MATERIALS. , 2002, , .		1
183	Proposal of Flexible Atomic and Molecular Process Management for Monte Carlo Impurity Transport Code Based on Object Oriented Method. Contributions To Plasma Physics, 2002, 42, 157-162.	1.1	0
184	Analysis of Detached Recombining Plasmas by Collisional-Radiative Model with Energetic Electron Component. Contributions To Plasma Physics, 2002, 42, 419-424.	1.1	3
185	Fluctuation Characteristics in Detached Recombining Plasmas Journal of Plasma and Fusion Research, 2002, 78, 1093-1101.	0.4	2
186	Static and dynamic behaviour of plasma detachment in the divertor simulator experiment NAGDIS-II. Nuclear Fusion, 2001, 41, 1055-1065.	3.5	185
187	Influence of Plasma Resistance and Fluctuation on Probe Characteristics in Detached Recombining Plasmas. Contributions To Plasma Physics, 2001, 41, 473-480.	1.1	37
188	Title is missing!. Journal of Materials Science, 2001, 36, 5169-5175.	3.7	9
189	2-D PIC Simulation on Space-Charge Limited Emission Current from Plasma-Facing Components. Contributions To Plasma Physics, 2000, 40, 478-483.	1.1	8
190	Simulation on Structure and Dynamic Behavior of Dust Particles in a Direct Current Plasma-Sheath. Journal of Plasma and Fusion Research, 1999, 75-CD, 234-257.	0.4	0
191	Prospect on the Atomic and Molecular Processes in Plasmas 5. Recent Topics in Experiments 5.1 Molecular Activated Recombination Processes in Divertor Plasmas. Journal of Plasma and Fusion Research, 1999, 75, 1162-1168.	0.4	1
192	Various Phenomena on PSI. PSI in Fusion Devices. Edge Plasma Physics and Atomic-Molecular Processes Journal of Plasma and Fusion Research, 1999, 75, 378-383.	0.4	0
193	Anomaly of Langmuir Probe Characteristics in Detached Recombining Plasmas. Contributions To Plasma Physics, 1998, 38, 31-37.	1.1	33
194	Numerical Simulation on Structure of Detached Helium Plasmas with Hydrogen and Helium Gas Puff in NAGDISâ€II. Contributions To Plasma Physics, 1998, 38, 55-60.	1.1	8
195	Enhancement of Plasma Heat Flow to the Conductive Divertor Plate Associated with Crossâ€Field Potential Variation and Thermoelectron Emission. Contributions To Plasma Physics, 1998, 38, 349-354.	1.1	4
196	Simulation and experiment on detached plasmas in the linear divertor simulator NAGDIS-II. European Physical Journal D, 1998, 48, 127-136.	0.4	3
197	Particle simulation on multiple dust layers of Coulomb cloud in cathode sheath edge. European Physical Journal D, 1998, 48, 239-244.	0.4	2
198	Experimental Evidence of Molecular Activated Recombination in Detached Recombining Plasmas. Physical Review Letters, 1998, 81, 818-821.	7.8	130

#	Article	IF	CITATIONS
199	Heat flows through plasma sheaths. Physics of Plasmas, 1998, 5, 2151-2158.	1.9	44
200	Confinement and structure of electrostatically coupled dust clouds in a direct current plasma–sheath. Physics of Plasmas, 1998, 5, 3517-3523.	1.9	48
201	Numerical Simulation Study on Density Dependence of Plasma Detachment in Simulated Gas Divertor Experiments of The TPDâ€I Device. Contributions To Plasma Physics, 1996, 36, 339-343.	1.1	15
202	Particle in Cell Simulation on Thermoelectron Emission from Hot Target Plate. Contributions To Plasma Physics, 1996, 36, 386-390.	1.1	14
203	Suppression of secondary electron emission from the material surfaces with grazing incident magnetic field in the plasma. Physics of Plasmas, 1996, 3, 4310-4312.	1.9	17
204	Nonlinear interactions between high heat flux plasma and electronâ€emissive hot material surface. Physics of Plasmas, 1996, 3, 281-292.	1.9	28
205	Three-dimensional microscopic analysis of inter-laminar area in cross-ply laminate using a homogenization theory. , 0, , .		0